Automated calculation of optical monitoring strategy based on use of sensitive wavelengths and error self-compensation effects

Lucas Arsac, Fabien Lemarchand, Detlef Arhilger, Harro Hagedorn, Julien Lumeau

▶ **To cite this version:**

Lucas Arsac, Fabien Lemarchand, Detlef Arhilger, Harro Hagedorn, Julien Lumeau. Automated calculation of optical monitoring strategy based on use of sensitive wavelengths and error self-compensation effects. Optics Express, 2025, 33 (20), pp.42028. ⟨10.1364/oe.573002⟩. ⟨hal-05348151⟩

HAL Id: hal-05348151

https://amu.hal.science/hal-05348151v1

Submitted on 5 Nov 2025

HAL is a multi-disciplinary open access archive for the deposit and dissemination of scientific research documents, whether they are published or not. The documents may come from teaching and research institutions in France or abroad, or from public or private research centers.

L'archive ouverte pluridisciplinaire **HAL**, est destinée au dépôt et à la diffusion de documents scientifiques de niveau recherche, publiés ou non, émanant des établissements d'enseignement et de recherche français ou étrangers, des laboratoires publics ou privés.

Copyright - All rights reserved

Research Article | Vol. 33, No. 20 / 6 Oct 2025 / Optics Express 42028
Optics EXPRESS

Automated calculation of optical monitoring strategy based on use of sensitive wavelengths and error self-compensation effects

LUCAS ARSAC,[1,2] FABIEN LEMARCHAND,[1] DETLEF ARHILGER,[3] HARRO HAGEDORN,[3] AND JULIEN LUMEAU[1,*]

[1]Aix Marseille Univ, CNRS, Centrale Med, Institut Fresnel, Marseille, France
[2]Bühler SAS, Paris, France
[3]Bühler Leybold Optics GmbH, Alzenau, Germany
[*]julien.lumeau@fresnel.fr

Abstract: Defining an appropriate optical monitoring strategy is critical to ensure accurate layer thicknesses in thin-film optical filter fabrication. This work focuses on active monochromatic monitoring combined with level-cut layer termination. We propose a method that limits monitoring wavelength changes while still selecting high-sensitivity wavelengths for each layer. This approach minimizes individual thickness errors and simultaneously preserves inter-layer error self-compensation. The method was validated on multiple examples of non-quarter-wave filters. Compared to existing strategies, it offers a practical balance between accuracy, robustness, and ease of implementation.

© 2025 Optica Publishing Group under the terms of the Optica Open Access Publishing Agreement

1. Introduction

Definition of an appropriate monitoring strategy is a crucial point in the manufacturing process of thin-film optical filters as it directly impacts the deposited layers' thicknesses accuracy and so the component final spectral response. Among others, optical monitoring is a commonly employed technique to control the deposited layers' thicknesses, which consists of measuring in real time the evolution of the filter transmittance versus the deposited thickness [1]. Depending on the type of optical monitoring system (OMS) used, transmittance measurement can be monochromatic or broadband, both possessing their own assets and drawbacks depending on the desired application and the system used [2,3]. For example, broadband monitoring has generally remarkable low sensitivity to random errors in measurement [4], whereas monochromatic monitoring may offer higher sensitivity at specific wavelengths, an interesting feature for narrow bandpass applications [5,6]. A review of the various types of monochromatic monitoring is presented in [2]. In this paper, we focus exclusively on what is defined in [2] as active variable-wavelength monochromatic monitoring, namely, we allow ourselves to change the monitoring wavelength during process if needed (variable-wavelength monitoring) and we employ algorithms embedded in the OMS for online correction of layer termination instant (active monitoring). Other types of monochromatic monitoring mentioned in [2] are outside the scope of our study. The method investigated here allows the use of on-line correction algorithms during deposition and permits changes to the monitoring wavelength when necessary. Specifically, we use here level-cut monitoring [1,7], i.e. layer termination is based on absolute transmittance measurements, applied on non-quarter-wave filters. Turning-point monitoring approach, generally used for quarter-wave mirrors and narrow bandpass filters [4–6] was not investigated here as it generally does not require extensive strategy determination.

Various methods have been developed to minimize error accumulation by selecting optimal monitoring wavelengths. In [8], they search for the most sensitive wavelength (MSW) of each layer, i.e. the wavelength maximizing the derivative of the monitoring signal $\partial T/\partial d$ at the layer

#573002 https://doi.org/10.1364/OE.573002
Journal © 2025 Received 11 Jul 2025; revised 20 Aug 2025; accepted 12 Sep 2025; published 24 Sep 2025

Optics EXPRESS

termination instant, with T the transmittance and d the deposited thickness. The influence of previous layers' thickness errors was also taken into account in [9] while searching for sensitive monitoring wavelengths. In a previous study [10], we also investigated the change of the monitoring wavelength for each layer, in order to select the one that is expected to result in the lowest thickness error. High-performance filters were produced with this method.

However, these methods require frequent changes in the monitoring wavelength, which can diminish the effectiveness of the error self-compensation effect [11]. Indeed, it is generally admitted that optically monitoring multiple consecutive layers at the same wavelength is advantageous since it enables the use of the error self-compensation effect, which reduces the impact of cumulative thickness errors [12]. For this reason, conventional monitoring strategies generally aim to minimize wavelength changes, reserving them for specific situations, such as after a test-glass change to manage error accumulation or when the current wavelength could induce significant thickness errors on a particular layer. Yet, the choice of monitoring wavelength(s) for those conventional monitoring strategies is often quite arbitrary or based on empirical rules.

It is practically impossible to achieve error-free thicknesses when depositing layers due to the intrinsic limitations of coating machines [13,14]. This means that previously mentioned methods [8–10], which aim to minimize thickness errors but do not allow for efficient error compensation, unless additional complex error-compensation algorithms are implemented in OMS, are inherently limited. Error accumulation will likely become significant at some point, potentially harming filter performance.

From this analysis, we developed a new method that strives to change as few as possible the monitoring wavelength during process, while selecting those monitoring wavelengths based on their high sensitivity. Hence, we minimize deposited thickness errors on each individual layer and at the same time, unlike other methods, we leverage error compensation effects from active on-line correction algorithms of our monitoring system. This approach is compatible with any commercially available optical monitoring setup, since the monitoring strategy is fully calculated prior to deposition. As a result, no real-time monitoring wavelength adjustment or complex software modifications are required.

2. Limitations of direct optical monochromatic monitoring

2.1. Technical limitations

Direct optical monochromatic monitoring, especially in the case of non-quarter-wave stack with level-cut monitoring, is known to show some important error accumulation effect [9]. Throughout the entire process, both coating machine and monitoring system induce random and systematic thickness errors [13–15], due among others to OMS detector noise, OMS on-line signal processing, variation of the materials deposition rate, shutter delay at the instant of the layer termination, or even spatially non-uniform and inhomogeneous layer deposition.

Thickness production errors can even be greater if the monitoring wavelength is not thoroughly selected by the operator. For instance, the spectral resolution of the system might limit the accuracy of the transmittance measurement if the monitoring occurs in a spectral region with sharp transmittance peaks. Also, monitoring system detector noise is spectrally dependent and should be taken into account. For a given layer termination, variation of transmittance with respect to thickness increase is influenced by the selected monitoring wavelength. All those features should be considered when determining the monitoring spreadsheet of a multilayer stack.

2.2. Common monochromatic monitoring approach

Classical monochromatic monitoring approach implies the use of a single (or very few) wavelength(s) for the filter fabrication monitoring. One generally tries to find a single wavelength to monitor all the layers, but as the number of layers of the filter increases, this becomes gradually

Optics EXPRESS

more difficult if even possible. In that case, one could use one (or very few) additional monitoring wavelength(s) for the process but, overall, it is commonly accepted that changing as few as possible the monitoring wavelength appears desirable [12]. An interesting method was presented in [11] to automatically generate a monochromatic monitoring spreadsheet with no (or barely no) wavelength change, based on practical requirements on the monitoring signal shape. Overall, although filters with satisfactory performance can be manufactured, the choice of the monitoring wavelength is rather an acceptable compromise for all the layers more than an optimal solution, so thickness errors will be likely produced for some layers.

To partially counterbalance the previously committed thickness errors, efficient algorithms for level-cut on-line correction [15–17] can be used. They allow to some extend to reduce the effect of error accumulation, but depending on the thin film design, it was shown that with increasing number of layers to be monitored on one monitoring glass position the latter effect is not negligible anymore and unequivocally decrepits the final filter performances [18]. Hence, the monitoring glass has to be changed but then comes other issues due to indirect optical monitoring, because the deposited thickness on the monitoring glass can differ from the one on the desired component and calibration factor is therefore required [14,16]. Moreover, this calibration factor is not necessarily constant during deposition and may have to be corrected in real time with retro-engineering algorithm [19]. However, not all coating machines have the appropriate configuration to implement such retro-fitting solution.

Finally, deciding when to change the monitoring glass is another open issue with little to no literature on the topic. Up to now, this decision relies entirely on the experience of the thin-film designer as no dedicated algorithm yet exist.

2.3. Alternative polychromatic approach

Reducing deposited thickness errors is a major challenge in thin-film manufacturing, and one effective approach is to limit the accumulation of these errors during the deposition process. Various studies have proposed algorithms to address this issue, many of which are based on the MSW method [8–10]. These algorithms determine an optimal wavelength for each layer, minimizing the error accumulation effect. However, such strategies inherently require frequent changes in monitoring wavelength which can prevent the use of on-line correction algorithms, such as quasi-swing [20] or POEM [17] algorithms, that allow efficient error self-compensation.

Another approach to error mitigation involves designing several different layer stacks for a given optical transmittance target and, for a given production environment, select the one with the highest manufacturability [21]. Such computational simulations combining design and monitoring strategy pairs have emerged as a powerful tool for manufacture process of optical filters, enabling the realization of high-quality optical components [22–24]. These simulations reveal critical process parameters but are constrained by their complexity and computational cost, requiring simplifications to remain practical [24]. Also, they require perfect knowledge of the manufacturing tools and all associated random and systematic errors, which is generally not the case.

2.4. Novel method: balancing sensitivity and error compensation

Building on these efforts, we propose a method inspired by Zideluns et al. [10] that seeks to minimize monitoring wavelength changes unless the optical signal becomes unsuitable. Our approach groups consecutive layers into subgroups, assigning a single monitoring wavelength to each subgroup to reduce the frequency of wavelength changes. While this method may not limit error accumulation as effectively as some other MSW-based methods, it enables the use of on-line correction algorithm, leveraging error self-compensation effects over multiple layers. Although not detailed here, experimental tests were performed both with and without activation of on-line correction algorithm, on different optical functions. Results clearly showed that activating

Optics EXPRESS

such algorithm during deposition significantly reduced average thickness errors compared to experiments without it, demonstrating a pronounced error self-compensation effect.

This method differs fundamentally from both conventional monochromatic monitoring and MSW-based approaches. Traditional monochromatic monitoring begins with a single wavelength and introduces additional wavelengths only when no compromise can be achieved for all layers. MSW-based approaches aim to select for each layer the most promising monitoring wavelength which generally implies to change it for every layer.

In contrast, our method starts with multiple sensitive wavelengths and consolidates them, identifying common wavelengths that can be used across several layers to minimize changes. It strives to balance sensitivity and stability by maintaining the same wavelength over several layers.

Combining error-sensitive monitoring wavelengths with active correction algorithms has been shown to reduce cumulative errors [8,25]. However, these advanced methods often do not rely on direct readouts of experimental monitoring signal features, such as amplitude or turning point values. Instead, they use these features to perform additional complex dynamic calculations. For instance, they recalculate during process the admittance of the multilayer stack for real-time adjustment of the termination instant [25], provided the layer signal offers two turning points - which is not always feasible due to thin layers and the use of long monitoring wavelengths. Generally, these online admittance calculation methods are not integrated into conventional commercial monitoring software and must be implemented in the OMS, which can be technically demanding. Furthermore, the reliance on advanced algorithms and complex computations for real-time adjustments can make these approaches resource-intensive, potentially limiting their practical application.

In our approach, we retain error self-compensation by minimizing wavelength changes and employing on-line trigger point correction algorithms during manufacturing, that are based on direct information from monitoring signals, such as layer signal starting point, turning point if there are some, and termination level. Instead of actively eliminating accumulated errors, we focus on mitigating their effects to delay divergence.

This paper introduces a practical framework for generating monitoring spreadsheets tailored to specific optical filter designs. Unlike other approaches, our method does not require prior optimization of error self-compensating designs or additional software modification of monitoring system. The monitoring strategies are entirely calculated before the deposition process. They appear to be efficient enough to prevent premature thickness error accumulation and, therefore, does not require any dynamic adjustment of the monitoring wavelength during the deposition course. This simplicity allows operators of any expertise to manufacture multi-layer stacks using standard thin-film coating machine, provided the design is available.

3. Development of automated algorithm for monitoring strategy determination

3.1. General method presentation

The approach developed here consists of monitoring as many consecutive layers as possible at the same monitoring wavelength, using sensitive wavelength according to [10] method. Monitoring multiple consecutive layers at the same wavelength allows the use of on-line correction algorithm to correct layer termination transmittance level, because the monitoring system has access to previous transmittance extremum values.

Determining if a monitoring wavelength is suitable for a given layer is not a trivial task. Yet, it exists some good rules of thumb that tell if a monitoring wavelength will likely induce important thickness error and be clearly not appropriate for the monitoring the current layer. Hence, before seeking for the most promising monitoring wavelengths, our method pre-eliminates all the supposedly inappropriate monitoring wavelengths of each layer. For instance, it typically includes cases where the layer termination would occur extremely close to the next or previous turning point, or if the total signal amplitude is severely low. Then, among the remaining wavelengths,

Optics EXPRESS

the algorithm seeks for sensitive monitoring wavelengths in common between consecutive layers to pack them into subgroups.

The physical quantities examined by our criteria, for the preliminary elimination of unsuitable monitoring wavelengths, are similar to the ones in [10,11]. Stricter criteria result in more wavelengths being excluded upfront, leaving fewer wavelengths shared among consecutive layers. To address this, we loosened the criteria, removing only the most clearly inappropriate wavelengths while retaining a broader set, including both promising and less optimal wavelengths. Description of the four used criteria is detailed below:

- Start amplitude (SA): it corresponds to the absolute transmittance variation between the beginning of the layer and the first turning point of the signal. If the start amplitude is too low, i.e. the first turning point is too close after the beginning of the layer, then OMS might miss the turning point due to signal noise which could lead in wrong deposited thickness. Start amplitude should be at least 1% from experiments.

- Swing Out (SO): it corresponds to the signal amplitude between last turning point and the end of the layer, divided by the theoretical total amplitude A of the signal (see eq.1). Hence, swing value is evaluated between 0 and 100%. If the layer signal ends right after the last turning point, swing value will be close to 0%, while it will be close to 100% if the layer ends right before the next virtual turning point. Minimal swing out value should be above 2% and below 80%. Starting the layer right after a turning is surely not optimal, but terminating the layer close to the next virtual turning point can lead to huge thickness errors and should be definitely avoided.

$$SO = \frac{|T_{lastTP} - T_{end}|}{A} \tag{1}$$

- Bandwidth (BW): the OMS is based on a monochromator with a given spectral resolution, typically between 0.5 and 8 nm. As a result, the OMS transmittance measurement is actually averaged over a finite spectral range. If there is a significant variation in transmittance within this resolution range, it will induce an error in the OMS transmittance measurement, impacting the final deposited thickness. This criterion aims to check that the discrepancy between theoretical and simulated signal is lower that a given threshold, at the beginning of the layer, at end of the layer and at the turning point(s), for a given monitoring wavelength. Typically, we want an absolute transmittance difference below 0.1%.

- Turning Point (TP) presence: it checks whether OMS simulated signal has an extremum or not. This is only checked for the first layer after a wavelength change (see Section 3.2), otherwise it is not mandatory. The existence of a turning point on the first layer after a wavelength change enables OMS to perform an online correction of the layer termination with greater precision.

3.2. Algorithm architecture

For each individual layer in the investigated stack, the method begins with a preliminary elimination of unsuitable wavelengths based on the four binary criteria outlined in Section 3.1. Following this step, each layer is associated with a vector of remaining wavelengths, to which the algorithm assigns a merit function value M_i (see Eq. (2)). The merit function, adapted from [10], differs slightly from the original MSW method [8]. It takes into account the derivative of transmittance with respect to the deposited thickness at the current layer's termination point, as well as the derivative of transmittance with respect to the thickness of previously deposited layers at the same wavelength. Essentially, the merit function prioritizes monitoring wavelengths that are highly sensitive to thickness errors in the current layer while being relatively insensitive to

Optics EXPRESS

errors in previously deposited layers. This approach aims to reduce the correlation of thickness errors during the process and prevent premature error accumulation [9]. For the following explanation of the algorithm structure, let us note:

– S_i : the set of suitable monitoring wavelengths for the i-th layer

– σ_i^p: the intersection of the sets from S_i to S_p (see Eq. (3))

– $M_\mathrm{i}(\lambda)$: the merit value of the i-th layer, at wavelength λ (see Eq. (2))

– $\frac{\partial T}{\partial d_i}(\lambda)$: the derivation of transmittance with respect to deposited thickness, at wavelength λ

– $\Delta T_{noise}(\lambda)$: the spectral noise of the OMS

– α, β : weighting coefficients

$$M_i(\lambda) = \frac{1}{\left|\frac{\partial T}{\partial d_i}(\lambda)\right|} * \left[\alpha * \sum\nolimits_{1 \le j \le i-1} \frac{1}{(i-1)} * \left|\frac{\partial T}{\partial d_j}(\lambda)\right| + \beta * \Delta T_{noise}(\lambda)\right] \tag{2}$$

$$\sigma_i^p = \bigcap_{k=i}^{p} S_k \tag{3}$$

The weighting coefficients α and β control the balance between sensitivity to thickness errors and robustness to the OMS noise in the selection of monitoring wavelengths. They were established experimentally from various realizations of different optical functions. In practice, they should be adjusted according to the characteristics of the optical monitoring setup, in order to reasonably balance sensitivity to thickness errors against robustness to noise in the selection of monitoring wavelengths.

After every wavelength of each layer is being attributed their merit value (see Eq. (2)), the algorithm calculates the intersection of each consecutive set of suitable wavelength (see Eq. (3)), starting with layer-1, and iterate until an empty set of wavelengths is obtained. If σ_p is empty but $\sigma_{\mathrm{p}-1}$ was not, then the layers from 1 to (p-1) are monitoring with the wavelength that is in the non-empty set $\sigma_{\mathrm{p}-1}$. If this set contains several potential wavelengths, we compute for all those wavelengths the arithmetic mean of their merit value, from layer 1 to (p-1). The wavelength providing the lowest mean merit value over the (p-1) layers is chosen as the monitoring wavelength.

To better understand the algorithm procedure, let us consider an example of a 10-layer beamsplitter studied in section 4. The algorithm found a 2-wavelength strategy for this filter, with one wavelength monitoring the first 7 layers of the stack. Table 1 shows how our method selected the monitoring wavelength 450 nm, among 5 remaining candidates. Indeed, 450 nm presents the lowest mean merit function (MF) value across the 7 first layers, even if for individual layers 1, 5, 6 and 7, other wavelengths had lower merit values. This approach prioritizes overall performance over the subgroup rather than layer specific sensitivity.

Once the monitoring wavelength is selected for layers 1 to (p−1), the algorithm moves to the next layer p and repeats the process. It calculates the intersection of suitable wavelengths for consecutive layers starting from p, identifying a new subgroup until the maximum number of packed layers is reached or the intersection becomes empty. If multiple wavelengths remain at the end of this process, the one with the lowest mean merit value is again selected. By following this iterative procedure throughout the entire stack, the algorithm identifies monitoring wavelengths for multiple consecutive layers, minimizing wavelength changes while maintaining sensitivity.

Optics EXPRESS

Table 1. example of choice of monitoring wavelengths by the algorithm, for the first 7 layers of a beamsplitter

Suitable monitoring wavelength, nm	435	440	446	**450**	453
MF layer 1	0.428	0.367	0.290	0.237	**0.234**
MF layer 2	3.149	3.025	2.851	**2.719**	2.753
MF layer 3	0.726	0.721	0.705	**0.688**	0.720
MF layer 4	1.810	1.559	1.304	**1.151**	1.117
MF layer 5	0.908	0.738	0.573	0.480	**0.449**
MF layer 6	**1.638**	1.734	1.978	2.286	2.849
MF layer 7	**0.643**	0.674	0.694	0.695	0.738
Mean MF	1.329	1.260	1.199	**1.179**	1.266

3.3. *Discussion of algorithm parameters*

For a given layer, choosing the wavelength with the lowest merit function value, as done in [10], ensures the use of a relevant monitoring wavelength that is more likely to minimize thickness errors. However, this does not imply it is the only suitable wavelength for monitoring. As demonstrated by our method, our algorithm utilizes groups of wavelengths with relatively low, though not necessarily minimal, merit values for each individual layer. Despite this, we achieve filters with relatively low committed thickness errors. This underscores that while the merit value is a valuable indicator for selecting monitoring wavelengths, it is not an absolute measure. There must be other unknown parameters, not accounted for in our merit function, that explain why effective control strategies can be achieved even with wavelengths that do not have the strict minimum merit function among all candidates.

One would also notice that, depending on the binary criteria selectivity, the number of suitable wavelengths for each layer will be different and it will be more or less difficult to find some wavelength in common. As a result, if we use restrictive criteria, each layer will have very few monitoring wavelengths indicated as suitable, so the intersection of the sets Si will quickly be empty as we iterate along the layer stack, and so the average number of consecutive layers that we will be able to monitor at the same wavelength will be relatively low (this is somewhat the approach that was implemented in [10] work). On the contrary, if we use relaxed criteria, the average number of consecutive layers monitored at the same wavelength will be much higher and it is then important to implement the merit value calculation to select the best wavelength.

To define the algorithm's criteria values, we initially set them based on our experience and previous work [10]. For instance, we considered a monitoring signal acceptable if its SO value falls within the range of [20, 80] %, if its SA value exceeds 4%, and if it contains at least one TP. However, these criteria do not account for the bandwidth limitations of the OMS system or the impact of thickness errors from previous layers on the current layer.

While these initial criteria produce visually satisfactory monitoring signals, they proved too restrictive for our method, as they eliminated too many wavelengths, making it difficult to group a large number of consecutive layers under the same monitoring wavelength. For example, in the 51-layer multi-bandpass filter (MBPF) presented in Section 4.6, the calculated monitoring strategy required 17 different wavelengths, resulting in wavelength changes every 3 layers, on average. When performing monochromatic optical monitoring, it is generally admitted that limiting wavelength changes is more desirable, as well as choosing monitoring wavelength close to the spectral region of the filter application. Depending on the application, one can typically use the same monitoring wavelength for 20 to more than 50 layers, which is very far from the outcome on 51-layer MBPF with [10] criteria. To address this issue, we relaxed the criteria as

Optics EXPRESS

much as possible while still maintaining acceptable monitoring signal shapes, ultimately reducing the frequency of wavelength changes. The final criteria values used in our study are as follows: SO must be within [2, 90] %, SA must exceed 1%, and TP is mandatory only after a wavelength change.

For the sake of clarity, we do not provide an exhaustive study of all the different tested criteria values and their impact on our experimental results. The proposed criteria are those that were implemented throughout this study and that allowed determining efficient optical monitoring strategies. However, in some specific cases, especially if it proves to be difficult to find monitoring wavelength that can be associated with a large number of layers, adapting these parameters might be necessary. That said, further relaxing the criteria beyond the previously mentioned thresholds would likely lead to thickness errors too large for the algorithm to fully compensate them, eventually degrading the final spectral response of the filter. For instance, if the SA amplitude is lower than 1%, the OMS may incorrectly detect the layer's first turning point due to detector noise, resulting in severe thickness errors. Similarly, if the SO value approaches 100%, the same issue could arise, possibly leading to incorrect TP value measurement or, even worse, missing the TP presence detection.

4. Experimental applications

4.1. Setup presentation

Optical filters were manufactured with plasma assisted reactive magnetron sputtering (HELIOS400) and monitoring system OMS5100 from Bühler Leybold Optics company. This coating machine is equipped with a rotating turntable upon which the sample is placed. Solid target materials to sputter are positioned above the sample, as is the light source of OMS5100. With each turntable rotation, a transmittance measurement is performed when the sample passes under the light source. Transmitted light is collected beneath the sample by an optical fiber connected to OMS5100. Rotation speed was set to 240 rpm and deposition rate of high and low index materials are respectively around 0.41 and 0.47 nm.s-1, so that a measurement is performed approximatively every 0.1 nm thickness increment.

The layers are deposited using plasma-assisted reactive magnetron sputtering [26]. This process employs a mid-frequency dual magnetron setup with metallic targets that are oxidized thanks to radio-frequency plasma source. Spectral measurements are performed ex-situ using a Perkin Elmer Lambda 1050 spectrophotometer.

A variety of designs with different complexity and sensitivity to thickness errors was fabricated. For all those designs, the previously described procedure was systematically applied.

High and low index materials utilized during process were respectively Nb2O5 and SiO2 whose refractive index table are shown in Fig. 1 and 2 (imaginary part not displayed). Fused Silica 7980 glass substrates were mainly used, expect for the AR coating that was deposited on B270 substrate. If change of monitoring test glass was ever needed during a deposition, Fused Silica 7980 was also used as monitoring glass. The usable spectral range for the optical monitoring was set to [400, 1100] nm to maintain acceptable signal to noise ratio.

4.2. Optical functions studied

As mentioned in section 1, we only tested non-quarter-wave filter designs with the algorithm, as for quarter-wave mirrors and quarter-wave bandpass filters some straightforward and well-known monitoring strategies already exist [6,27,28]. Three main types of filters with gradual complexity were tested here. Their designs are summarized in Table S1 (see Supplement 1).

We started investigating optical functions with flat broadband response, first a 50/50% beamsplitter (BS) and then an antireflective (AR) coating. Such filters have limited sensitivity to thickness errors. Indeed, committed thickness errors will likely create some moderate ripples

Optics EXPRESS

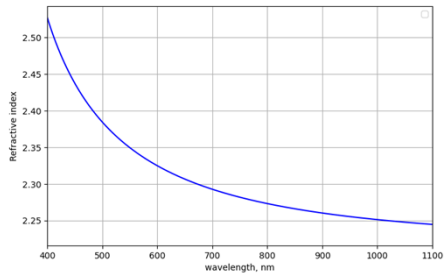

Fig. 1. Nb2O5 refractive index (real part).

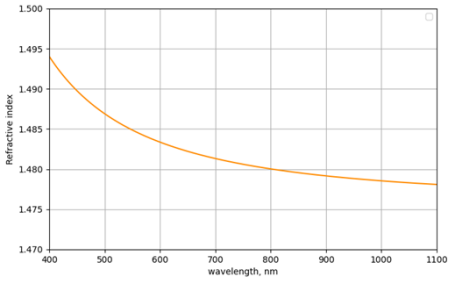

Fig. 2. SiO2 refractive index (real part).

around the target transmittance level, as well as slight spectral shift but, because of their broad and flat spectral response, the resulting filter function will be quite similar.

Then, we tested a non-quarter design with slowly and gradually varying transmittance following a triangular shape (triangular filter, TF). Typically, its transmittance linearly increases and then decreases from 30 to 100% over 200 nm spectral regions (see section 4.3.). For this filter, layers thickness errors will quickly induce ripples and deviation from the triangular transmittance target. Also, unlike previous flat broadband functions, the centering of the filter becomes now an important feature regarding the appreciation of the quality of filter production, although this spectral centering is not a main issue due to the limited design complexity.

Finally, we studied a multi-bandpass filter (MBP) and a Notch filter (NF), that have sharp variations of spectral responses. For those filters, even slight thickness errors can drastically impact the expected level of transmittance in the bandpass of those filters, as well as their good centering

4.3. Experimental results application

To better understand the sensitivity of each filter design to thickness errors and evaluate the quality of the produced components, we conducted Monte-Carlo simulations of thickness errors on the layers of the designs. Simulating a coating process is inherently complex due to its multi-parameter nature, and it is challenging to account for all parameters accurately. However, by estimating the impact of the primary sources of thickness errors, we can gain valuable insights into a filter's sensitivity.

In our simulation framework, we only considered physical thickness errors and excluded refractive index errors. We did not account systematic errors, induced for example by shutter delays or mechanical mispositioning of the substrate holder, but instead accounted random errors caused by OMS signal noise or fluctuations in temperature, vacuum pressure, or target power. We attributed thickness random relative errors to online correction algorithms and thickness

Optics EXPRESS

random absolute errors to photometric inaccuracies. For each design, we simulated N = 1000 filters, incorporating both random relative and absolute thickness errors.

Ideally, systematic errors in refractive index should also be considered, as there is an inevitable error when characterizing a material's refractive index before using it in the coating process. However, estimating such errors is challenging because they likely depend on the characterization method, the material nature, and are probably wavelength-dependent. For this reason, we chose to ignore those systematic errors. Regarding random refractive index errors, due to magnetron sputtering process known stability, we excluded them.

The Monte-Carlo simulations were performed over the region of interest of each filter with a 0.2 nm step, providing sufficient spectral resolution for thick stacks with sharp transmittance variations. A normal distribution was used to model the thickness deviation of each layer, input parameters are summed up in Table 2. In the next sections, for each studied filter, we will display over its region of interest the following curves: experimental response of the component, theoretical response and a 2-sigma confidence interval (CI) around theory, containing 95% of the simulated filters.

Table 2. input parameters for Monte-Carlo error simulations

	Mean, μ	Standard deviation, σ
Absolute thickness error, nm	0	0.3 to 0.5
Relative thickness error, %	0	0.1
Absolute index error, no unit.	0	0
Relative index error, %	0	0

4.4. *Beamsplitter (BS)*

The experimental application of our strategy determination algorithm was initially tested on a 10-layer beamsplitter filter. Its theoretical transmittance is $50 \pm 0.5\%$ over the [400, 800] nm visible spectral range. For this example, the algorithm calculated a 2-wavelength strategy with 449 nm for layers (1-7) and 983 nm for the layers (8-10). Figure 3 shows the experimental response of the filter and Monte-Carlo error simulation ($\sigma = 0.3$ nm) as a comparison. We can estimate the produced thickness errors to be lower than equivalent random thickness errors of 0.3 nm.

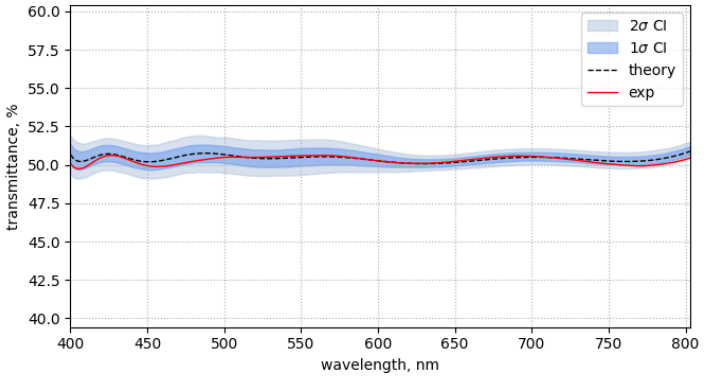

Fig. 3. Comparison of experimental response of 10-layer BS with Monte-Carlo error simulation ($\sigma = 0.3$ nm, N = 1000).

Optics EXPRESS

4.5. Antireflective coating (AR)

The next tested filter was an 8-layer broadband antireflective coating, deposited on both side of a B270 glass. Its theoretical transmittance is 98.5 ± 0.5% over [400, 900] nm. Just like the BS example, such flat broadband function is not too sensitive to layer thickness errors. We can still achieve high transmittance value with moderate produced thickness errors, as underlined on Fig. 4 by the 1σ confidence interval around theoretical response.

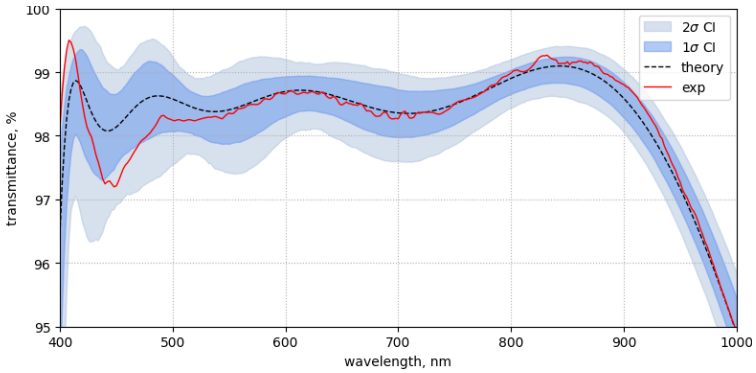

Fig. 4. Comparison of experimental response of 8-layer AR with Monte-Carlo error simulation (σ = 0.8 nm, N = 1000).

For this example, the algorithm calculated a 2-wavelength strategy with 494 nm for layers (1-3) and 400 nm for the layers (4-8). Figure 4 presents the experimental response of the filter and Monte-Carlo error simulation (σ = 0.8 nm) as a comparison. Calculated strategy provided satisfactory results as reflectance remains below 3.0% over wide [400, 950] nm range. We can estimate the produced thickness errors to be lower than random thickness errors of 0.8 nm.

4.6. Triangular filter

We next fabricated a 20-layer triangle filter, whose transmittance linearly increases from 30 to 100% over [400, 600] nm and then decreases to 30% over [600, 800] nm. Accurate centering of this filter is now important, unlike previous broadband application, and is impacted by produced thickness errors.

For this example, the algorithm calculated a monochromatic strategy with all the layers monitored at 402 nm. Figure 5 presents the experimental response of the filter and Monte-Carlo error simulation (σ = 0.3 nm) as a comparison. Calculated strategy provided satisfactory results with experimental curve fitting within ± 1.5% transmittance corridor around theory. We can estimate the produced thickness errors to be lower than random thickness errors of 0.3 nm.

4.7. Multi-bandpass filter

To further test our algorithm, we manufactured a 51-layer multi-bandpass filter, whose layer physical thicknesses are between 30 and 255 nm (see Annex 1). Each bandpass has a theoretical transmittance of 96% and a FMWH of 8 nm. They are respectively centered at 500, 550 and 600 nm. Rejection band is over [470, 630] nm with transmittance lower than 0.02%.

For this filter, the algorithm calculated a 5-wavelength strategy. Figure 6 presents the experimental response of the filter and Monte-Carlo error simulation (σ = 0.4 nm) as a comparison. Calculated strategy provided highly satisfactory experimental results, with T > 92.5% for each bandpass. Spectral shift of the 3 three bandpass are respectively -0.4, -0.6 and -0.3 nm. Based on simulations, we estimated the produced thickness errors for this filter to be equivalent to random thickness errors of 0.4 nm.

Optics EXPRESS

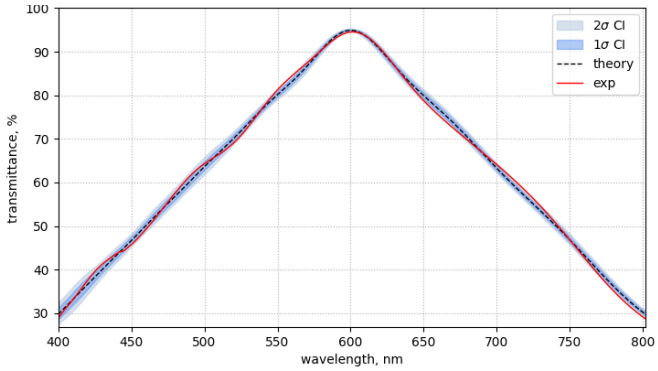

Fig. 5. Comparison of experimental response of 20-layer TF with Monte-Carlo error simulation (σ = 0.3 nm, N = 1000).

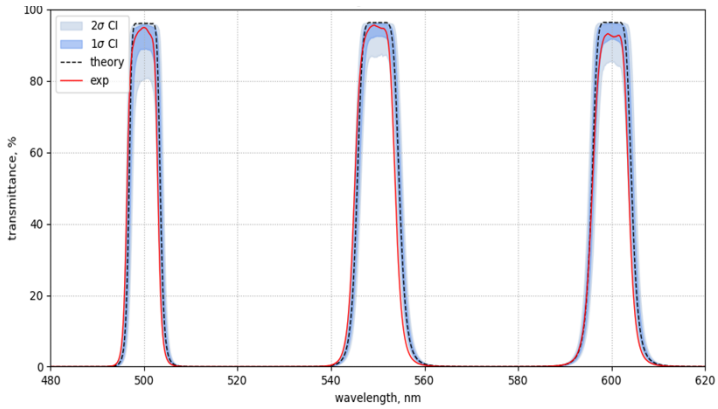

Fig. 6. Comparison of experimental response of 51-layer MBPF with Monte-Carlo error simulation (σ = 0.4 nm, N = 1000).

It is worth noting that, due to spectral shift, the experimental curve of the center bandpass is slightly out of the 2σ confidence interval (see Fig. 7), although closely matching the target maximum transmittance value. If the errors produced during deposition were purely random, then a spectral shift would be generally accompanied by a significant drop in transmission within the bandpass. Since this is not the case here, as we are very close to the theoretical maximum transmission, we can conclude that systematic errors (possibly of refractive index) were produced during deposition, inducing this spectral shift. This highlights the limitations of our random error simulation method for filters with steep edges, where their centering is critical.

Given that our experimental curve is shifted according to the theory, it would be necessary to simulate random errors greater than 0.4 nm for the experimental curve to fall within the confidence interval CI. However, due to the difficulty in precisely estimating the causes and magnitude of these systematic errors, we chose to exclude them from our Monte-Carlo simulations and use the latter to provide a qualitative estimate of the filter's successful realization.

4.8. Notch filter

Finally, we tested our algorithm on a 75-layer notch filer, whose layer physical thicknesses typically range from 30 to 450 nm (see Annex 1). Theoretical transmittance is greater than 95%

Optics EXPRESS

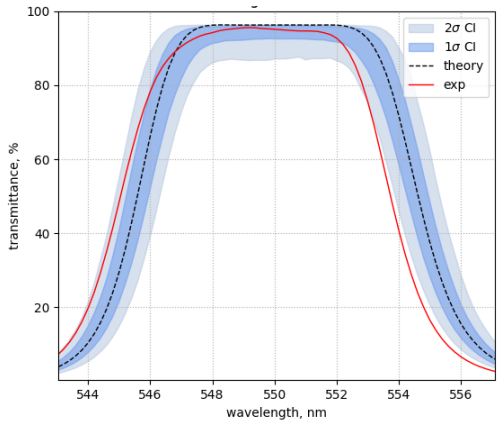

Fig. 7. Zoom on transmittance curve of the 550 nm bandpass of 51-layer MBPF, comparison of experiment and Monte Carlo error simulation (σ = 0.4 nm, N = 1000).

over [470, 500] and [520, 560] nm ranges. Cut-off band centered at 510 nm has a FWHM of 13 nm and goes down to 0.3% of transmittance at minimum.

No efficient optical monitoring strategy could be found after simulation when using a single test glass due to the large number of layers. To overcome this limit, we adjusted the algorithm to calculate a strategy with 3 different monitoring test glasses. It determined 8 monitoring wavelengths in total, respectively 2, 3 and 3 for each test glass. The splitting of the filter was done manually, every 25 layers or so, so that the freshly changed test glass would not start with a low refractive index layer and that the optical monitoring signal of first layer would have a decent amplitude. Figure 8 and 9 shows the experimental curve and Monte-Carlo simulation (σ = 0.3 nm) as a comparison. Despite the large number of layers, strong agreement between experiment and theory was achieved, with T > 94% in the bandpass and a spectral shift lower than 0.1 nm for the cut-off band. Based on simulations, we can estimate the produced thickness errors for this filter to be equivalent to random thickness errors of 0.3 nm.

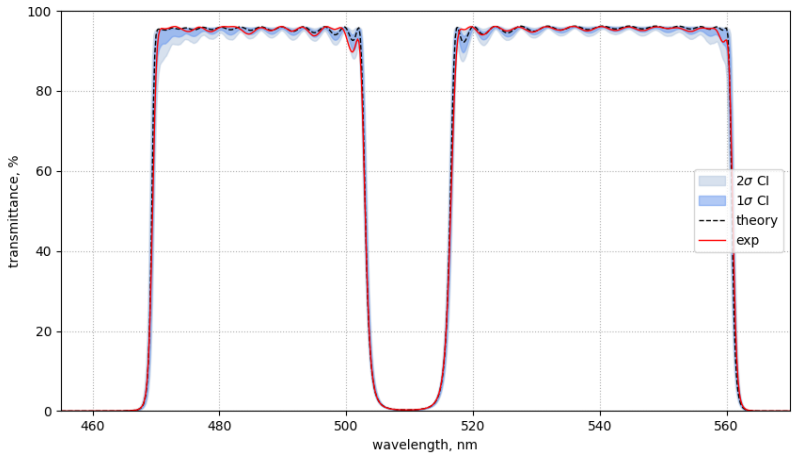

Fig. 8. Comparison of experimental response of 75-layer NF with Monte-Carlo error simulation (σ = 0.3 nm, N = 1000).

Optics EXPRESS

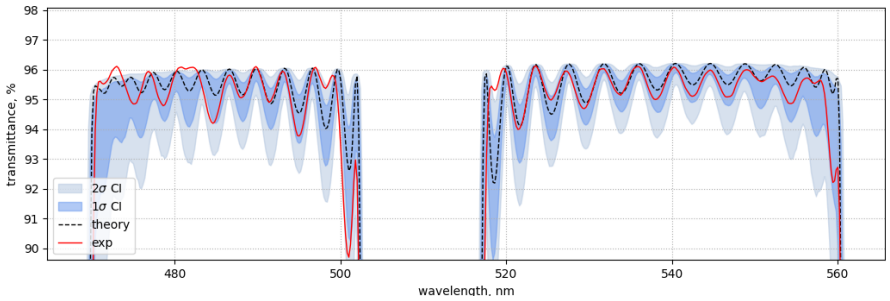

Fig. 9. Zoom on the top of the 2 transmission bands of 75-layer NF, comparison between experiment and Monte-Carlo error simulation ($\sigma = 0.3$ nm, $N = 1000$)

5. Conclusion

We developed a novel algorithm to determine suitable monitoring wavelengths for subgroups of layers within a given filter design. Building on the principles of the MSW method, our approach shifts the focus from identifying the optimal wavelength for each individual layer to finding relatively sensitive wavelengths that can be shared across several consecutive layers. By excluding wavelengths likely to cause poor layer termination accuracy, the algorithm ensures robust monitoring. Unlike the traditional MSW method, our approach supports the use of on-line trigger point correction algorithms, enabling error self-compensation during deposition. This reduces the impact of cumulative thickness errors and improves the stability of the entire manufacturing process, as depicted by the various successful practical realizations.

We experimentally validated our technique across a range of optical functions with increasing complexity, such as broadband antireflective coating, beamsplitter or Notch filter. The strong agreement between theoretical response and experimental results underlines the efficiency and versatility of our approach.

Disclosures. The authors declare that there are no conflicts of interest related to this article.

Data availability. Data underlying the results presented in this paper are not publicly available at this time but may be obtained from the authors upon reasonable request.

Supplemental document. See Supplement 1 for supporting content.

References

1. H. A. Macleod, "Monitoring of optical coatings," Appl. Opt. **20**(1), 82 (1981)..
2. A. V. Tikhonravov, M. K. Trubetskov, and T. V. Amotchkina, "Optical monitoring strategies for optical coating manufacturing," in *Optical Thin Films and Coatings*, Elsevier, (2018, pp. 65–101.
3. A. V. Tikhonravov, M. K. Trubetskov, and T. V. Amotchkina, "Investigation of the error self-compensation effect associated with broadband optical monitoring," Appl. Opt. **50**(9), C111 (2011).
4. A. V. Tikhonravov and M. K. Trubetskov, "Automated design and sensitivity analysis of wavelengh-division multiplexing filters," Appl. Opt. **41**(16), 3176 (2002).
5. P. Bousquet, A. Fornier, R. Kowalczyk, *et al.*, "Optical filters: Monitoring process allowing the auto-correction of thickness errors," Thin Solid Films **13**(2), 285–290 (1972).
6. H. A. Macleod, "Turning Value Monitoring of Narrow-band All-dielectric Thin-film Optical Filters," Opt. Acta Int. J. Opt. **19**(1), 1–28 (1972).
7. F. Zhao, "Monitoring of periodic multilayers by the level method," Appl. Opt. **24**(20), 3339 (1985).
8. C.-C. Lee, K. Wu, C.-C. Kuo, *et al.*, "Improvement of the optical coating process by cutting layers with sensitive monitor wavelengths," Opt. Express **13**(13), 4854–4861 (2005).
9. A. V. Tikhonravov, M. K. Trubetskov, and T. V. Amotchkina, "Statistical approach to choosing a strategy of monochromatic monitoring of optical coating production," Appl. Opt. **45**(30), 7863 (2006).
10. J. Zideluns, F. Lemarchand, D. Arhilger, *et al.*, "Automated optical monitoring wavelength selection for thin-film filters," Opt. Express **29**(21), 33398 (2021).
11. M. Trubetskov, T. Amotchkina, and A. Tikhonravov, "Automated construction of monochromatic monitoring strategies," Appl. Opt. **54**(8), 1900 (2015).

Optics EXPRESS

12. A. Tikhonravov, Iu. Lagutin, A. Lagutina, *et al.*, "Advanced algorithms for monochromatic monitoring of complex optical coatings," Appl. Opt. **62**(30), 7904 (2023).
13. A. Macleod, "Optical coatings from design through manufacture", Thin Film Center Inc., training manual (2010).
14. B. T. Sullivan and J. A. Dobrowolski, "Deposition error compensation for optical multilayer coatings. 1.Theoretical description," Appl. Opt. **31**(19), 3821–3835 (1992).
15. A. Zöller, M. Boos, H. Hagedorn, *et al.*, "Computer simulation of coating processes with monochromatic monitoring," presented at the *Optical Systems Design*, N. Kaiser, M. Lequime, and H. A. Macleod, eds., Glasgow, Scotland, United Kingdom, Sep. 2008, p. 71010G.
16. A. Zoeller, M. Boos, R. Goetzelmann, *et al.*, "Substantial progress in optical monitoring by intermittent measurement technique," presented at the *Optical Systems Design 2005*, C. Amra, N. Kaiser, and H. A. Macleod, eds., Jena, Germany, Sep. 2005, p. 59630D.
17. R. R. Willey, "Simulation comparisons of monitoring strategies in narrow bandpass filters and antireflection coatings," Appl. Opt. **53**(4), A27 (2014).
18. A. V. Tikhonravov, M. K. Trubetskov, and T. V. Amotchkina, "Computational experiments on optical coating production using monochromatic monitoring strategy aimed at eliminating a cumulative effect of thickness errors," Appl. Opt. **46**(28), 6936 (2007).
19. Jinlong Zhang, Chong Cao, Alexander V. Tikhonravov, *et al.*, "Advantages and challenges of optical coating production with indirect monochromatic monitoring," Appl. Opt. **54**(11), 3433 (2015).
20. I. V. Kochikov, Yu. S. Lagutin, A. A. Lagutina, *et al.*, "Stable Method for Optical Monitoring the Deposition of Multilayer Optical Coatings," Comput. Math. Math. Phys. **60**(12), 2056–2063 (2020).
21. A. V. Tikhonravov, M. K. Trubetskov, T. V. Amotchkina, *et al.*, "Key role of the coating total optical thickness in solving design problems," presented at *the Optical Systems Design*, C. Amra, N. Kaiser, and H. A. Macleod, eds., St. Etienne, France, 2004, p. 312.
22. A. V. Tikhonravov and M. K. Trubetskov, "Computational manufacturing as a bridge between design and production," Appl. Opt. **44**(32), 6877 (2005).
23. T. V. Amotchkina, S. Schlichting, H. Ehlers, *et al.*, "Computational manufacturing as a key element in the design–production chain for modern multilayer coatings," Appl. Opt. **51**(31), 7604 (2012).
24. A. V. Tikhonravov, M. K. Trubetskov, T. V. Amotchkina, *et al.*, "Estimations of production yields for selection of a practical optimal optical coating design," Appl. Opt. **50**(9), C141 (2011).
25. A. V. Tikhonravov and M. K. Trubetskov, "Elimination of cumulative effect of thickness errors in monochromatic monitoring of optical coating production: theory," Appl. Opt. **46**(11), 2084 (2007).
26. M. Scherer, "Magnetron sputter-deposition on atom layer scale," Vak. Forsch. Prax. **21**(4), 24–30 (2009).
27. A. V. Tikhonravov, M. K. Trubetskov, and T. V. Amotchkina, "Optical monitoring strategies for optical coating manufacturing," in *Optical Thin Films and Coatings* pp. 62–93 (Elsevier, 2013).
28. T. Begou, F. Lemarchand, F. Lemarquis, *et al.*, "High-performance thin-film optical filters with stress compensation," J. Opt. Soc. Am. A **36**(11), C113 (2019).

185.104.138.84 2025-09-29 10:13:2